Turkish Journal of Physics

http://journals.tubitak.gov.tr/physics/

Research Article

Turk J Phys
(2018) 42: 484 – 493

doi:10.3906/fiz-1805-4

Investigation of the optical properties of the liquid crystal-based devices via Mueller matrix formalism

Ömer POLAT*
Department of Electrical and Electronics Engineering, Faculty of Engineering and Natural Sciences, Bahçeşehir University, İstanbul, Turkey

Received: 08.05.2018 • **Accepted/Published Online:** 09.07.2018 • **Final Version:** 15.08.2018

Abstract: A model approach for the Mueller matrix (MM) of the twisted nematic liquid crystal spatial light modulator (TNLC-SLM) was proposed. In the first part of the study, the MM of the TNLC cell in the absence of applied voltage was investigated both theoretically and experimentally. In the second part, the model approach was improved by considering the reorientation of both tilt and azimuth angles of the liquid crystal (LC) molecules in the presence of applied voltage. Comparison of the theoretical MM elements with the experimental ones from the literature showed that, instead of decaying exponentially, the azimuth angle rotates with respect to the cell walls in a critical voltage range before the molecules are completely untwisted. It also pointed out that the effect of the tilt and the azimuth angles of the molecules on the optical properties of the light travelling in the LC cell could change depending on the polarization state of the input light and the voltage applied to the cell.

Key words: Spatial light modulators, liquid crystals, Mueller matrix, light polarization

1. Introduction

Twisted nematic liquid crystal (TNLC) cells are devices that are widely used in technology as the backbone of several electro-optic (EO) devices. TNLC-based light modulators designed to modulate both the amplitude and the phase of the light are called spatial light modulators (SLM) [1–3]. If an SLM acts as a phase modulator, it modulates only the phase of the light, and the intensity of the light remains unchanged. However, if it acts as an amplitude modulator, it modulates only the amplitude of the light, and the phase of the light remains unchanged. Liquid crystal displays (LCD) are amplitude modulators mostly used as displays in laptops, TVs, cellphones, and tablets for years [4–7]. The other kind of modulators, phase modulators, have applications such as electrically controlled lenses [8–10], optical tweezers [11,12], laser beam shaping [13,14], 3D holographic displays [15], and laser wavelength control [16,17].

A TNLC cell consists of liquid crystal (LC) molecules sandwiched between the reference glass surfaces. In the cell, the LC molecules twist from one glass surface to the other. That twist structure causes the modulation in the polarization state of the light travelling in the cell. When the light with an arbitrary polarization state enters the cell, it changes its polarization to another state after it exits the cell depending on the parameters such as optical anisotropy of the LC molecules, wavelength of the input light twisting angle of the molecules, and the thickness of the cell. For example, if the LC cell has a 90° twist from one glass surface to the other, linearly horizontally polarized input light changes its polarization state to vertical. Besides, an external electric

*Correspondence: omer.polat@eng.bau.edu.tr

field can also be applied to the cell to change the polarization state of the light to any desired state. In the case of the applied filed, because the dielectric torque created by the electric field overcomes the elastic torque between the LC molecules, the twist structure of the molecules are deformed and all LC molecules tend to align in the direction of the applied field and the long axis of the LC molecules becomes perpendicular to the glass surfaces in the cell (homeotropic state). Tuning the voltage applied between the glass surfaces of the LC cell, one can modulate the light travelling through the cell.

Model approaches presented in recent studies [1,6,18] showed that in TNLC-based EO devices, the retardance of the LC cell is inversely proportional to the tilt angles of the molecules. Under the influence of the increasing voltage applied to the cell, depending on the tilt angle reorientation, retardance of the molecules decreases and finally reaches zero while the LC cell changes its state from twisted to homeotropic. Theoretical results obtained from these model approaches were in accordance with the experimental measurements in which linearly polarized light could be controlled changing from the horizontally to the vertically (and vice versa) polarized after it exits the cell. However, for a complete analysis of the light travelling through the untwisting LC cell having any state of polarization (especially elliptically and circularly polarized), not only the reorientation of the tilt angle but also the azimuth angle of the molecules should be taken into account.

In a recent study about the polarization modulation of the twisted nematic spatial light modulator (TNSLM), Kapil et al. measured experimentally that the azimuth angle of the LC director close to the glass surface of the TNSLM changed smoothly from 37° to 71° before it abruptly changed to -45° at a critical grayscale value addressed on it [19]. In another research, Lin et al. presented the distributions of the twist angle and the tilt angle of the LC director across the width of the TNLC cell as function of applied voltage [20]. As the voltage increased, the azimuth angle of the director shifted to higher angles. Similar results were also reported in [21].

This result reveals that more investigations should be made on the tilt as well as the azimuth angles of the LC molecules of TNSLMs and on how the reorientation of the molecules affects the polarization properties of the travelling light before they undergo state change.

For this purpose, polarization properties of the travelling light in TNLC-based devices depending on the reorientation of the molecules were investigated by means of the Mueller matrix (MM) formalism. In the first part of the study, the MMs of TNLC were modelled in the absence of voltage applied to the LC cell. The validity of the model was checked comparing the results with the theoretical light transmission data from a recent study and the data of the MM elements of LCD from the experiment were performed in our lab. In the second part, a model approach was developed to explore the behavior of the MM elements under the influence of the applied voltage. Three different scenarios were proposed for the reorientation of the azimuth angle of the molecules. Comparison of our theoretical results with the experimental ones from the literature showed that, in some critical voltage range, before the LC molecules are completely untwisted, the behavior of the azimuth angle of the LC molecules is more significant than that of the tilt angle and could explain the polarization properties of the elliptically and circularly polarized light travelling in the cell.

2. General aspects of the MM formalism

Polarized light travelling through the TNLC cell can be expressed mathematically by means of the Mueller formalism [22–24]. In this formalism, the MM of the TNLC is represented by a 4×4 matrix having sixteen elements, which defines the response of the optical media to all the possible polarization states of the input light. LC molecules, which are aligned in an LC cell, act like linear optical retarders [25] and are mathematically

represented by an MM. MM elements of the LC can be extracted by using some experimental techniques. As indicated in [26,27], experimentally, sixteen elements of the MM representing the LC can be extracted by using linear and circular polarizers and/or analyzers at different configurations.

In Mueller formalism, the polarization state of the light is represented by a 4 × 1 matrix called the Stokes vector, with four components called I, Q, U, and V, where I is the total intensity and Q, U, and V are the differences between the intensity of horizontal and vertical, $+45^\circ$ and -45°, right-handed and left-handed polarized light respectively. Eq. (1) explains the overall mathematical interpretation of the MM showing the relation between the input and output polarization states after the interaction of the light within the medium:

$$\begin{bmatrix} I' \\ Q' \\ U' \\ V' \end{bmatrix} = \begin{bmatrix} m_{11} & m_{12} & m_{13} & m_{14} \\ m_{21} & m_{22} & m_{23} & m_{24} \\ m_{31} & m_{32} & m_{33} & m_{34} \\ m_{41} & m_{42} & m_{43} & m_{44} \end{bmatrix} \cdot \begin{bmatrix} I \\ Q \\ U \\ V \end{bmatrix} , \tag{1}$$

where 4 × 4 matrix is an MM of the optical media and m_{ij} is the individual matrix elements; I, Q, U, V and I', Q', U', V' are the Stokes vector components of the incoming and the outgoing light, respectively

2.1. Model approach for the MM of TNLC in the absence of applied voltage

We consider the MM of a planar cell (LC molecules align parallel to the cell walls) that can be given as a linear optical retarder as follows [25,28,29]:

$$MM(\delta,\theta) = \begin{bmatrix} 1 & 0 & 0 & 0 \\ 0 & \cos^2 2\theta + \cos\delta \sin^2 2\theta & (1-\cos\delta)\sin 2\theta \cos 2\theta & \sin\delta \sin 2\theta \\ 0 & (1-\cos\delta)\sin 2\theta \cos 2\theta & \sin^2 2\theta + \cos\delta \cos^2 2\theta & -\sin\delta \cos 2\theta \\ 0 & -\sin\delta \sin 2\theta & \sin\delta \cos 2\theta & \cos\delta \end{bmatrix}, \tag{2}$$

where θ is the azimuth angle of the LC molecules in the plane parallel to cell walls and δ is the phase retardation experienced by the light travelling through the cell. Because LC molecules change their orientation twisting from one layer to another in the cell, it is convenient to model LC cells as stacks of many planar LC layers having optical axis oriented at a specific azimuth angle, θ. Then, the MM of the twisted cell is:

$$M_{TNLC} = \frac{1}{N} \prod_{i=1}^{N} MM(\delta_i, \theta_i), \tag{3}$$

where N is the number of LC layers.

The validity of the model can be checked using the theoretical results given in the reference study [30] in which transmission curves of the light passing through the TNLC cell placed between the polarizers were calculated using the Jones Matrix (JM) model. In our approach, the LC cell was considered to have 180 layers (N = 180) and the azimuth angle of the LC molecules changes from one layer to another between 0° and 90° in the TNLC. Then, the transmission data were calculated using the following equation:

$$S_{out} = M(\psi_2).M_{TNLC}.M(\psi_1).S_{in}, \tag{4}$$

where S_{in} and S_{out} are the Stokes vectors of the input and output lights, respectively. In Figures 1a and 1b, the transmission data from the reference study are shown in comparison with the data from the MM model. The curves obtained from the MM model agree with those of the JM model and indicate that the model can be used for the MM studies of the TNLCs.

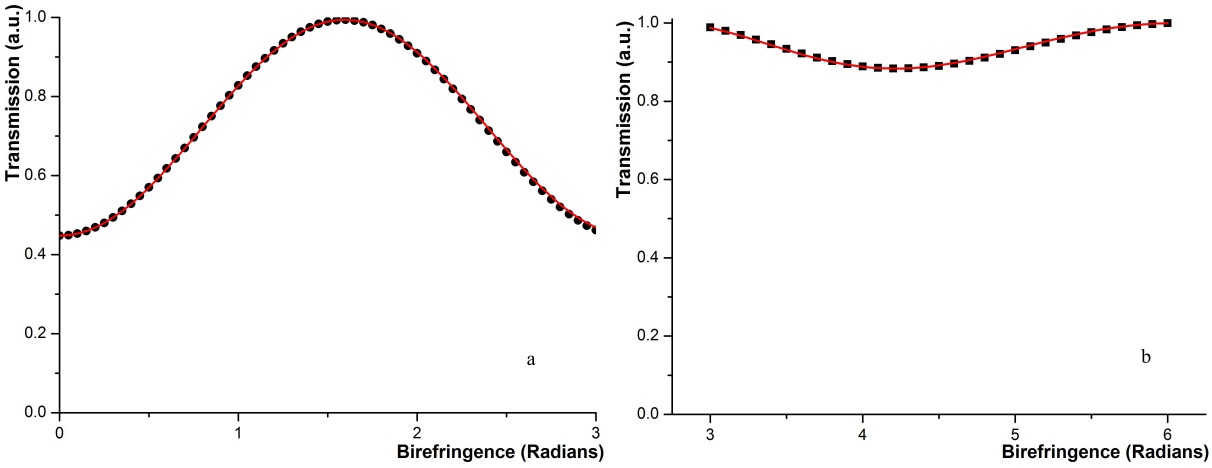

Figure 1. Transmission curves obtained from the JM (solid curves) and MM (filled circles) models for the polarizer angles: a) $\psi_1 = -25^\circ$ and $\psi_2 = -73^\circ$ in birefringence range from 0 rad to 3 rad and for b) $\psi_1 = 0^\circ$ and $\psi_2 = 90^\circ$ from 3 rad to 6 rad, respectively.

3. Comparison of the model with experimental results

In addition to the validation of the model as mentioned above, we also checked our model fitting the experimental curves of the MM elements obtained from the experiments. The MM elements of the TNLC cell were measured as a function of the wavelength of the input light by means of the experimental setup shown in Figure 2. In the LC cell, the alignment of the molecules twists from $+45^\circ$ to -45° with respect to x-axis.

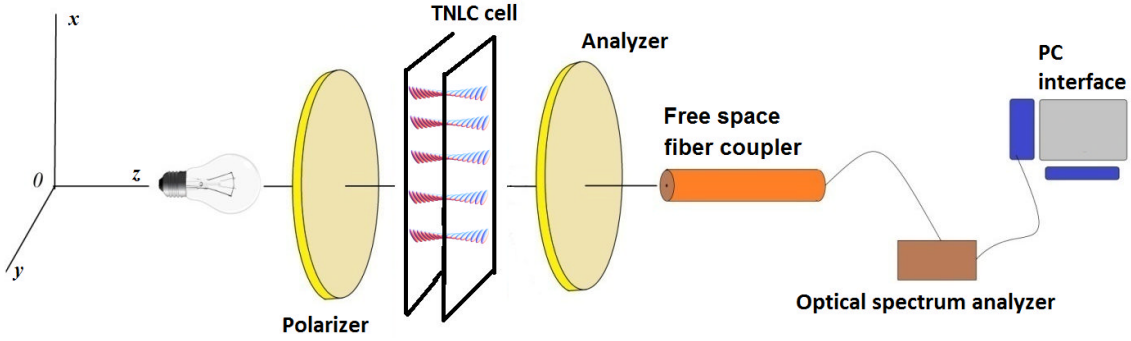

Figure 2. The layout of the experimental setup.

Light emerging from the broadband source passes through the polarizer, TNLC, and the analyzer and is detected by the optical spectrum analyzer. From the data of the light intensity, the MM elements of the TNLC were calculated using the technique explained in [26]. In Figure 3, plots of the elements versus wavelength are shown. Solid lines show the theoretical fits that were calculated using Eq. (4) taking the number of LC layers N = 180 and thickness of the cell d = 5 ?m. Wavelength-dependent optical anisotropy $\Delta n = \left[0.1518 + \frac{0.0034}{\lambda^2}\right]$ was substituted into the retardance term ($\delta = \frac{2\pi}{\lambda}\Delta nd$), and the azimuth angle of the molecules (θ) was assumed

to be changing from 45° to -45°. Successful fits of the curves showed that the model approach of MM of TNLC could explain the twisting characteristics of the LC molecules inside the cell. Besides, interpretations of the experimental MM curves could explain how the linearly polarized light changes its polarization state after exiting the cell. If the linearly polarized input light passes through the cell, the polarization state of the output light can be investigated by means of the first column (m_{11}, m_{21}, m_{31}, and m_{41}) and the second column elements (m_{12}, m_{22}, m_{32}, and m_{42}) [26,28]. As an example, for $\lambda = 650$ nm, the MM elements take the values of $m_{22} \approx 0.96$, $m_{23} \approx m_{32} \approx 0$, and $m_{33} \approx -0.78$. The value of m_{22} is very close to 1, and m_{23} and m_{32} are about zero, which means that horizontally or vertically polarized light travelling at this wavelength keeps its polarization state almost unchanged until it exits the cell.

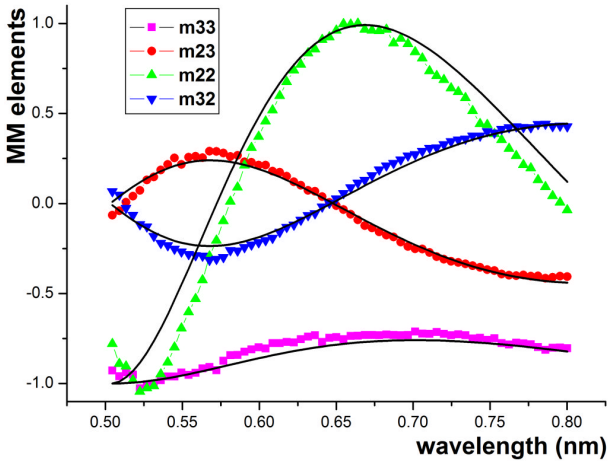

Figure 3. Experimental MM elements of TNLC as a function of the wavelength.

Another case is the output state of the 45° polarized input light that can also be checked comparing the first and the third column elements (m_{13}, m_{23}, m_{33}, and m_{43}). The value of the m_{33} indicates that at this wavelength (650 nm) the input light changes its polarization state to the elliptically polarized and its 45° polarized component becomes negative.

4. Model approach in the presence of applied voltage

As we mentioned above, the model approach of the MM of TNLC is successful in the absence of applied voltage. Making some modifications in the current model, a model for the MM of TNSLM can be proposed. In this section, we presented these modifications that are made in the model approach to explain the twist angle deformation of the LC molecules as well as the change in the polarization properties of the light travelling in the cell in the presence of applied voltage.

In our approach, TNSLM consists of 256 pixels and each pixel is subjected to different voltages. One of these pixels is illustrated in Figure 4. White pixel means that no voltage is applied to it and the LC molecules twist through the cell. In this case, light can pass without being blocked by the polarizers (crossed with respect to each other) mounted on both glass surfaces. Black pixel means that the voltage applied to the pixel is maximum and the LC molecules have already changed their state from twist to homeotropic. So, after passing through the polarizer-TNLC cell system, the light will be blocked when it reaches the second polarizer. In the range between the white and black pixels, different tones of gray are addressed because the light exits the second polarizer partially.

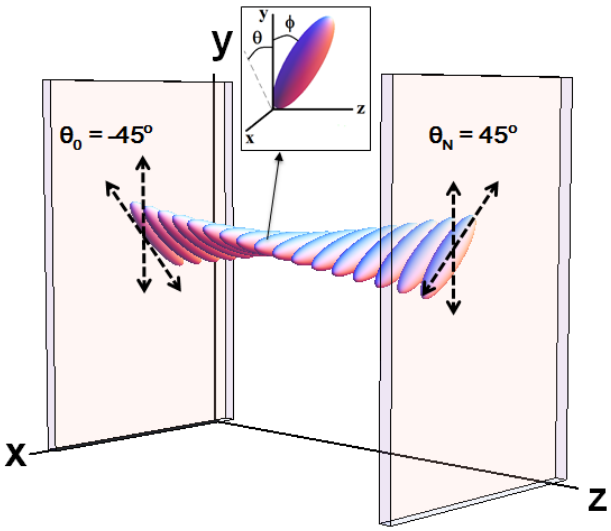

Figure 4. LC molecular orientation in one pixel in the absence of applied voltage. Azimuth and tilt angles of the LC molecule on the xy and yz planes, respectively.

For a complete analysis of the optical properties of the LC molecules, we defined two different angles as seen in Figure 4. The first one is the tilt angle (φ) that LC molecules make with respect to y axis in the yz plane. In the cell, when φ increases as a function of the applied voltage, because of being inversely proportional to the tilt angle, the retardance of the cell decreases according to the following equation:

$$\delta = \frac{\delta_0}{1 + \exp[-\xi(\eta p - \gamma)]}, \tag{5}$$

where ξ, γ, and η are the parameters that change depending on the LC molecules' structural properties. p shows the gray scale of the pixel mentioned above and it can take the values between 0 and 256 depending on the applied voltage. p = 0 and p = 256 correspond to black and white pixels, respectively.

The second one, azimuth angle (θ), defined as the angle of the LC molecules with respect to y axis in the xy plane. As θ changes from one molecule to another in the twisted LC cell, reorientation of θ of the ith molecule in the cell was defined as a function of θ_0, which is the azimuth angle of the molecules close to the glass surfaces of the cell:

$$\theta_i = -\theta_0 + \frac{i\pi}{2N}, \tag{6}$$

where N is the number of LC layers taken in the model. In our approach, three different scenarios for the reorientation of the θ_0 were proposed. Behavior of θ_0 with respect to the grayscale mode is given in Figure 5. In the first scenario, regardless of the applied voltage, θ_0 remains constant ($\pi/4$) and the LC cell keeps its twisted structure. In the second one, the LC cell starts to untwist at the grayscale mode p = 256 and turns completely into the homeotropic state at p = 0. In this scenario, θ_0 changes exponentially according to the following equation:

$$\theta_0 = \frac{\pi}{4}(1 - Exp[-\eta p]). \tag{7}$$

Finally in the third scenario, considering the experimental observations of the Kapil et al. [19] mentioned above

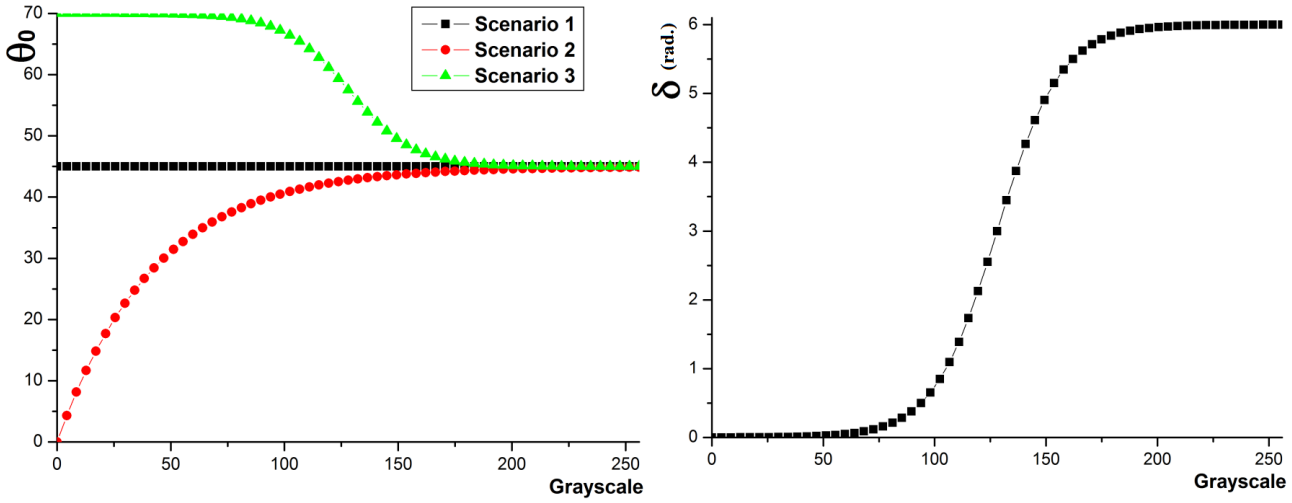

Figure 5. a) θ_0 and b) retardance (δ) as a function of the grayscale mode for three different scenarios. Retardance was assumed to have the same behavior in each scenario.

in the introduction, θ_0 was assumed to change exponentially from 45° up to 70°, instead it decays:

$$\theta_0 = \frac{5\pi/36}{1+\exp[\xi(\eta p-\gamma)]}+\frac{\pi}{4}. \tag{8}$$

Using Eqs. (5), (7), and (8) and taking the appropriate values of the constants $\gamma = 3$, $\xi = 3$, $\eta = 0.023$, and $\delta_0 = 6$, the azimuth angle and the retardance of the LC molecules versus grayscale are plotted in Figure 6. Then, choosing N = 900 and substituting the Eqs. (6), (7), and (8) into Eq. (3), a set of MM elements proposed for each scenario were calculated. The obtained results given in Figure 6 were compared with the experimental data of TNSLM (illuminated with 532 nm laser light) presented in [31]. As seen in Figure 6, m_{22} takes values between +1 to −1 as the grayscale changes from 0 to 256. This shows that the horizontally/vertically polarized input light changes its polarization state to vertical/horizontal. Another point is that the behavior of m_{22} curves change regardless of the reorientation of the azimuth angle in each scenario. From this, it can be noticed that the tilt angle reorientation of the molecules, which causes the change in the retardance, plays an important role in defining the characteristic of m_{22} as well as the optical properties of the horizontally/vertically linearly polarized input light. It is also shown that m_{22} does not give any information about how the azimuth angles of the molecules change and how the molecules untwist.

A similar analysis can be done for m_{33} by which ±45° linearly polarized input and output lights can be investigated. As seen in plots of m_{33}, like m_{22}, no significant change in the behavior of the curves was observed. Only the curve obtained from the third scenario shifts slightly from the others in the region between p = 100 and p = 150. With this analysis, it is pointed out that if the input and output lights are horizontally/vertically or ±45° polarized, the azimuth angle reorientation, as well as the deformation of the twist structure, does not matter for the light travelling in the cell. Only the reorientation of the tilt angle is important and can affect the state of polarization.

Contrary to m_{22} and m_{33}, the behavior of another diagonal element, m_{44}, gives the significant results about how the azimuth angle is reoriented inside the cell. m_{44} curves can be analyzed dividing the graphs into three regions. In the first region (between p = 150 and p = 256), it is inferred from the curves' characteristics

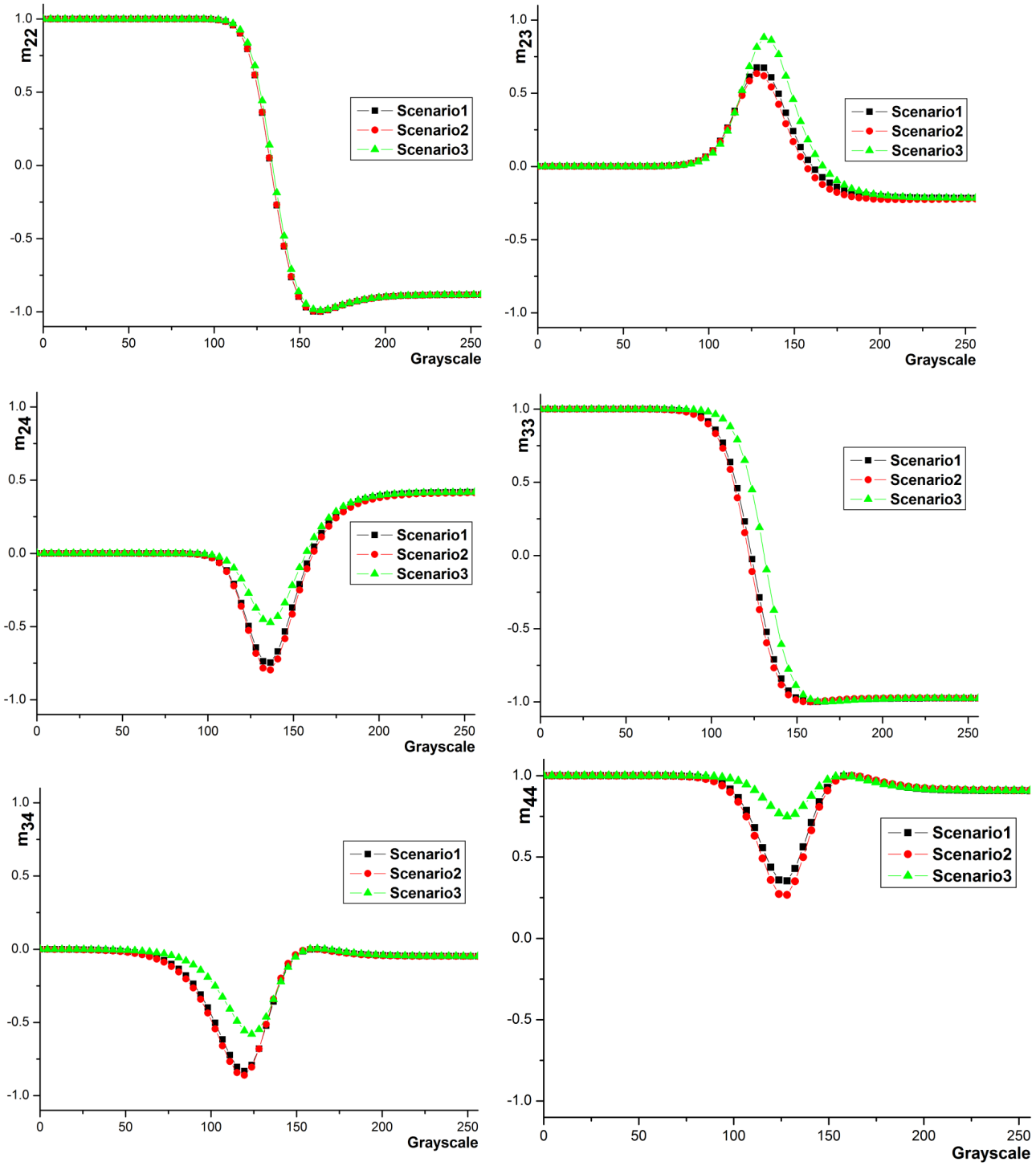

Figure 6. Plots of the theoretical MM elements of the TNSLM for each scenario suggested in the model approach.

that because of the weakness of the applied voltage to the cell no significant change in the tilt as well as the azimuth angles of the molecules occurs. In this region, theoretical curves obtained from each scenario are in agreement with the experimental ones given in [31]. In the second region (between p = 100 and p = 150),

the MM curves obtained from the third scenario, in which θ_0 changes between 45° and 70°, deviate from the curves obtained from the other two scenarios. According to the third scenario, as the voltage is increased, instead of starting to untwist, the LC molecules rotate in the xy plane. This rotation causes m_{44} not to change significantly and to take values close to 1 indicating that the circularly polarized input light somehow becomes elliptical.

However, according to other scenarios, m_{44} decreases more in that critical region indicating that the circularly polarized input light is expected to be more elliptical. This unexpected behavior of the LC molecules suggested in the third scenario shows a good agreement with the experimental curves. These results reveal an important character of the LC-based devices: the azimuth angle reorientation plays a more important role than that of the tilt angle on the optical properties of the light transmitted through the cell.

Finally, in the third region (between p = 100 and p = 0), it is clearly seen that the curves of all the plotted elements have the same behavior regardless of how the azimuth angles of the molecules change according to each scenario. At p = 0, as the LC molecules are completely untwisted and in homeotropic state, the diagonal MM elements have the value "1" while the nondiagonals have "0". The same behavior can be seen in the experimental MM curves. In that region, azimuth angle reorientation of the molecules does not play an important role in the behavior of the MM curves. It means that the torque created by the applied voltage overcomes the elastic torque which keeps the LC molecules in twist structure and causes LC molecules to untwist. As the retardance changes depending on the tilt angle of the molecules and takes the values close to zero, contrary to the second region, the tilt angle reorientation is more effective.

Our interpretation of the reorientation of the molecules from the behavior of m_{44} is also supported by other three nondiagonal elements (m_{23}, m_{34}, and m_{24}) demonstrated in Figure 6. In the same critical grayscale range, only the curves from the third scenario were found in agreement with the experimental curves. In the other voltage ranges, all the MM elements behave regardless of how the azimuth angles of the molecules change in each scenario.

In summary, from all of the comparisons discussed above we can infer that the model approach suggested for the TNLSM in which azimuth angles of the molecules decay exponentially is successful for the cases that the input and output lights are horizontally/vertically or $\pm 45^\circ$ linearly polarized. However, new scenarios are essential to explain the other forms, from linearly polarized to 45° polarized, linearly polarized to circularly polarized, 45° polarized to circularly polarized and vice versa.

5. Conclusion

A model approach was proposed for the MM of the TNLC to explain the behavior of the MM curves depending on the applied voltage that plays an important role in the polarization properties of the light transmitting through the TNLC and the performance of the EO device. The scenario proposed in the model approach for the azimuth angle reorientation of the LC molecules could explain the experimental MM curves of TNSLM presented in the literature. As the goal of the study, it was found out that, in addition to the current approaches in the literature about the modeling of the tilt angle reorientation, the proposed novel approach including the azimuthal angle reorientation that could explain the optical behavior of the circularly and elliptically polarized light is essential. Further study on new theoretical simulations and modelling should be conducted to find out which physical parameters of the LC molecules have a significant role in the molecules and how to control the rotation of the molecules just before they enter the untwisted state.

References

[1] Lu, K.; Saleh, B. E. A. *Opt. Eng.* **1990**, *29*, 240-246.

[2] Konforti, N.; Marom, E; Wu, S. T. *Opt. Lett.* **1988**, *13*, 251-253.

[3] Pezzaniti, J. L.; Chipman, R. A. *Opt. Lett.* **1993**, *18*,1567-1569.

[4] Zhibing, G.; Xinyu, Z.; Wu, T. X.; Wu, S. T. *J. Disp. Technol.* **2006**, *2*, 114-120.

[5] Ruibo, L.; Xinyu, Z.; Shin-Tson, W.; Qi, H.; Wu, T. X. *J. Disp. Technol.* **2005**, *1*, 3-14.

[6] Oh-e, M; Kondo, K. *Appl. Phys. Lett.* **1995**, *67*, 3895-3897.

[7] Bahadur, B. *Mol. Cryst. Liq. Cryst.* **1984**, *109*, 3-93.

[8] Nose, T.; Ishizaka, S.; Okano, K.; Fujita, N.; Murata, J.; Muraguchi, H.; Ozaki, N.; Honma, M.; Ito, R. In *SPIE Conference Proceedings: Emerging Liquid Crystal Technologies XII*, 28 January–2 February 2017; San Francisco, CA, USA, p. 8.

[9] Safrani, A.; Abuleil, M.; Isaac, S.; Solodar, A.; Klapp, I.; Kirzhner, M. G.; Abdulhalim, I. In *SPIE Conference Proceedings: Liquid Crystals XVIII,* 17–21 August 2014, San Francisco, CA, USA, p. 7.

[10] Perez-Vizcaino, J.; Mendoza-Yero, O.; Martinez-Cuenca, R.; Martinez-Leon, L.; Tajahuerce, E.; Lancis, J. *J. Disp. Technol.* **2012**, *8*, 539-545.

[11] Ni, J.; Wang, C.; Zhang, C.; Hu, Y.; Yang, L.; Lao, L.; Xu, B.; Li, J.; Wu, D.; Chu, J. *Light-Sci. Appl.,* **2017**, *6*, e17011.

[12] Kim, H.; Lee, W.; Ahn, J. In *Conference Proceedings: Lasers and Electro-Optics (CLEO)*, 14–17 May 2017, San Jose, CA, USA, p. 1.

[13] Solodar, A.; Klapp, I.; Abdulhalim, I. *Opt. Commun.* **2014**, *323*, 167-173.

[14] Kotova, S. P.; Mayorova, A. M.; Samagin, S. A. *J. Opt.* **2018**, *20*, 055604.

[15] Zhuang, Z.; Zhang, L.; Surman, P.; Song, W.; Thibault, S.; Sun, X. W.; Zheng, Y. *Appl. Optics* **2018,** *57*, 4457-4466.

[16] Huang, D.; Fan, W.; Cheng, H.; Xia, G.; Pei, L.; Li, X.; Lin, Z. *High Power Laser Science and Engineering* **2018**, *6*, e20.

[17] Xing-Xu, Z.; Lei, Q.; Ting-Yu, Z.; Rong-Sheng, Q. *Chinese Phys. B* **2018**, *27*, 054205.

[18] Soutar, C.; Lu, K. *Opt. E.* **1994**, *33*, 2704-2712.

[19] Dev, K.; Asundi, A. *Opt. Laser Technol.* **2013**, *47*, 323-328.

[20] Lin, H.-H.; Phan, Q.-H.; Lo, Y.-L.; *Opt. Express* **2015**, *23*, 10213-10223.

[21] Jin, H. C.; Yeon, H. L. *J. Opt. A* **2009**, *11*, 065709.

[22] Mueller, H. *Phys. Rev.* **1937,** *52*, 223-229.

[23] Mueller, H. *J. Appl. Phys.* **1935***, 6*, 179-184.

[24] Mueller, H. *Phys. Rev.* **1935**, *47*, 947-957.

[25] Berggren, E; Zannoni, C.; Chiccoli, C.; Pasini, P.; Semeria, F. *Phys. Rev. E* **1994**, *50*, 2929-2939.

[26] Bickel, W. S.; Bailey, W. M. *Am. J. Phys.* **1985**, *53*, 468-478.

[27] Firdous, S.; Ikram, M. In *Conference Proceedings: International Networking and Communication,* 11–13 June 2004, p. 115.

[28] Goldstein, D. *Polarized Light, Revised and Expanded*; Taylor & Francis, 2011.

[29] Yukitoshi, O. *Handbook of Optical Metrology*, CRC Press, 2009.

[30] Davis, J. A.; Moreno, I.; Tsai, P. *Appl. Optics* **1998**, *37*, 937-945.

[31] Stabo-Eeg, F.; Kildemo, M; Nerbo, I; Lindgren, M. *Opt. Eng.* **2008**, *47*, 073604.